



University
of Glasgow

Masson, R., Nicklin, S.A., Craig, M.A., McBride, M., Gilday, K., Gregorevic, P., Allen, J.M., Chamberlain, J.S., Smith, G.L., Graham, D., Dominiczak, A.F., Napoli, C. and Baker, A.H. (2009) *Onset of experimental severe cardiac fibrosis is mediated by overexpression of angiotensin-converting enzyme 2*. *Hypertension*, 53 (4). pp. 694-700. ISSN 0194-911X

<http://eprints.gla.ac.uk/6398/>

Deposited on: 10 August 2010

Hypertension

JOURNAL OF THE AMERICAN HEART ASSOCIATION



*Learn and Live*SM

Onset of Experimental Severe Cardiac Fibrosis Is Mediated by Overexpression of Angiotensin-Converting Enzyme 2

Rachel Masson, Stuart A. Nicklin, Margaret Anne Craig, Martin McBride, Kirsten Gilday, Paul Gregorevic, James M. Allen, Jeffrey S. Chamberlain, Godfrey Smith, Delyth Graham, Anna F. Dominiczak, Claudio Napoli and Andrew H. Baker

Hypertension 2009;53:694-700; originally published online Feb 16, 2009;

DOI: 10.1161/HYPERTENSIONAHA.108.122333

Hypertension is published by the American Heart Association, 7272 Greenville Avenue, Dallas, TX 75214

Copyright © 2009 American Heart Association. All rights reserved. Print ISSN: 0194-911X. Online ISSN: 1524-4563

The online version of this article, along with updated information and services, is located on the World Wide Web at:

<http://hyper.ahajournals.org/cgi/content/full/53/4/694>

Data Supplement (unedited) at:

<http://hyper.ahajournals.org/cgi/content/full/HYPERTENSIONAHA.108.122333/DC1>

Subscriptions: Information about subscribing to Hypertension is online at
<http://hyper.ahajournals.org/subscriptions/>

Permissions: Permissions & Rights Desk, Lippincott Williams & Wilkins, a division of Wolters Kluwer Health, 351 West Camden Street, Baltimore, MD 21202-2436. Phone: 410-528-4050. Fax: 410-528-8550. E-mail:
journalpermissions@lww.com

Reprints: Information about reprints can be found online at
<http://www.lww.com/reprints>

Onset of Experimental Severe Cardiac Fibrosis Is Mediated by Overexpression of Angiotensin-Converting Enzyme 2

Rachel Masson, Stuart A. Nicklin, Margaret Anne Craig, Martin McBride, Kirsten Gilday, Paul Gregorevic, James M. Allen, Jeffrey S. Chamberlain, Godfrey Smith, Delyth Graham, Anna F. Dominiczak, Claudio Napoli, Andrew H. Baker

Abstract—Angiotensin-converting enzyme (ACE) 2 is a recently identified homologue of ACE. There is great interest in the therapeutic benefit for ACE2 overexpression in the heart. However, the role of ACE2 in the regulation of cardiac structure and function, as well as maintenance of systemic blood pressure, remains poorly understood. In cell culture, ACE2 overexpression led to markedly increased myocyte volume, assessed in primary rabbit myocytes. To assess ACE2 function in vivo, we used a recombinant adeno-associated virus 6 delivery system to provide 11-week overexpression of ACE2 in the myocardium of stroke-prone spontaneously hypertensive rats. ACE2, as well as the ACE inhibitor enalapril, significantly reduced systolic blood pressure. However, in the heart, ACE2 overexpression resulted in cardiac fibrosis, as assessed by histological analysis with concomitant deficits in ejection fraction and fractional shortening measured by echocardiography. Furthermore, global gene expression profiling demonstrated the activation of profibrotic pathways in the heart mediated by ACE2 gene delivery. This study demonstrates that sustained overexpression of ACE2 in the heart in vivo leads to the onset of severe fibrosis. (*Hypertension*. 2009;53:694-700.)

Key Words: ACE2 ■ gene delivery ■ adeno-associated virus ■ hypertension ■ myocardium

Overactivity of the renin-angiotensin (Ang) system plays a fundamental role in the pathophysiology of hypertension and progression of heart failure.¹ Ang-converting enzyme (ACE) 2 is a recently identified homologue of ACE, and their catalytic domains share 42% amino acid identity.²⁻⁴ ACE2 expression is restricted to the heart, kidney, and testis.^{2,5} After myocardial infarction, increased ACE2 expression in the heart localized to vascular endothelium, smooth muscle, and cardiomyocytes in both rats and humans.⁶ Unlike ACE, ACE2 functions as a carboxypeptidase rather than a dipeptidyl carboxypeptidase⁵ and counterbalances the vasoconstrictor effects of ACE.⁷ ACE2 primarily hydrolyzes Ang II and, less efficiently, Ang I,² resulting in Ang 1-7 and Ang 1-9. Ang 1-9 is further hydrolyzed to Ang 1-7 by the actions of ACE.⁵ ACE inhibitors and Ang II receptor blockers are effective drugs for the treatment of cardiovascular diseases, as a result of blocking the vasoconstrictor, hypertrophic, and proinflammatory actions of Ang II.⁸⁻¹¹ Thus, ACE2 may play a pivotal role in the renin-Ang system by reducing concentrations of Ang II and raising levels of Ang 1-7.^{12,13} Therefore, manipulation of ACE2 activity has potential therapeutic use. However, ACE2 knockout mice have been associated with severe contractile dysfunction¹⁴ or, conversely, with no

observed effects on cardiac dimension or function.¹⁵ Overexpression of ACE2 by local delivery of lentivirus in the hearts of spontaneously hypertensive rats attenuated high blood pressure (BP) and perivascular fibrosis, reduced left ventricular (LV) wall thickness, and increased LV end diastolic and end systolic diameters.¹⁶ Conversely, transgenic overexpression of ACE2 in murine myocardium resulted in mild interstitial fibrosis and conduction disturbances leading to ventricular fibrillation, arrest, and sudden death.¹⁷

Gene delivery is a powerful approach to attenuate pathophysiological events.¹⁸ Recently, adeno-associated viruses (AAVs), in particular, AAV 6, 8, and 9, have emerged as promising cardiac gene transfer vectors.¹⁹⁻²¹ Here, we assessed the therapeutic potential of sustained overexpression of ACE2 on cardiac structure and function in stroke-prone spontaneously hypertensive rats (SHRSPs), an established recognized model of cardiovascular disease with genetic predisposition to essential hypertension and stroke sensitivity.²² Moreover, SHRSPs develop concentric LV hypertrophy²³ in response to BP elevation²³ that is evident at 12 weeks of age²⁴ and also display endothelial dysfunction.^{25,26} It is considered a valuable model because pathophysiological similarities to human disease exists, such as

Received August 29, 2008; first decision September 21, 2008; revision accepted January 15, 2009.

From the British Heart Foundation Glasgow Cardiovascular Research Centre (R.M., S.A.N., M.A.C., M.M., K.G., D.G., A.F.D., A.H.B.), Glasgow, United Kingdom; Senator Paul D. Wellstone Muscular Dystrophy Cooperative Research Centre (P.G., J.M.A., J.S.C.), University of Washington, Seattle; Faculty of Biological and Life Science (G.S.), University of Glasgow, Glasgow, United Kingdom; Sbarro Institute for Cancer Research and Molecular Medicine (C.N.), Temple University, Philadelphia, Pa; and the Department of General Pathology (C.N.), 1st School of Medicine, II University of Naples, Naples, Italy.

Correspondence to Andrew H. Baker, BHF GCRC, University of Glasgow, 126 University Place, Glasgow, G12 8TA United Kingdom. E-mail ab11f@clinmed.gla.ac.uk

© 2009 American Heart Association, Inc.

Hypertension is available at <http://hyper.ahajournals.org>

DOI: 10.1161/HYPERTENSIONAHA.108.122333

local factors for stroke,²⁷ and male SHRSPs maintain a higher BP than females.

Methods

These studies were approved by the home office according to regulations regarding experiments with animals in the United Kingdom.

Recombinant AAV6 and Recombinant AAV9 Vector Biodistribution and Transduction Efficiencies

Male 6-week-old SHRSPs were administered a single IV injection of recombinant AAV6 (rAAV6):CMVlacZ (2×10^{11} , 1.5×10^{12} , and 3×10^{12} viral particles [VP] per rat) in the presence or absence of recombinant human vascular endothelial growth factor (VEGF)-165 (20 μ g/100 g weight) or rAAV9:CMVlacZ at identical doses under general anesthesia (2% isoflurane, vol/vol). Two weeks postdelivery, DNA was extracted using the QIAmp DNA Mini kit (Qiagen). Real-time PCR was used to quantify vector genome particle number in tissue extracts. SyBr Green PCR core reagents kit (Applied Biosystems) with 200 nmol/L lacZ primers, forward (5'ATCTGACCACCAGC-GAAATGG3') and reverse (5'CATCAGCAGGTGTATCTGCCG3') amplified DNA under the following conditions: 95°C, 10 minutes; 95°C, 15 seconds; 60°C, 1 minute (50 cycles); 95°C, 15 seconds; 60°C, 15 seconds; and 95°C, 15 seconds. To assess β -galactosidase expression, 6- μ m sections were blocked in 20% swine serum before 1-hour incubation with anti- β -galactosidase antibody (MP Biomedicals). Sections were incubated with swine-anti-rabbit FITC antibody. For tissue and whole-limb staining, tissues were fixed in 2% paraformaldehyde before incubation in 5-bromo-4-chloro-3-indolyl β -D-galactoside stain (77 mmol/L of Na₂HPO₄, 23 mmol/L of NaH₂PO₄, 1.3 mmol/L of MgCl₂, 3 mmol/L of K₄Fe[CN]₆, and 0.05% [vol/vol] of 20 mg/mL 5-bromo-4-chloro-3-indolyl β -D-galactoside).

Assessment of Systolic BP

Four groups of animals (n=6 per group) were included in the rAAV6:ACE2 overexpression study: PBS, enalapril, rAAV6:human placental alkaline phosphatase (control vector, as characterized previously by Odom et al²⁸), and rAAV6:ACE2 (ACE2 cDNA was a kind gift from Mohan Raizada). Male 8-week-old SHRSPs received 3×10^{12} vp of either rAAV6:human placental alkaline phosphatase (hPLAP) or rAAV6:ACE2. Control animals were infused with 200 μ L of PBS, and enalapril was supplied in the drinking water at 0.1 mg/mL. Systolic BP monitoring was carried out weekly by computerized tail-cuff plethysmography.²⁴

Assessment of Cardiac Structure and Function by Echocardiography

Transthoracic echocardiography was performed using an Acuson Sequoia c512 ultrasound system with a 15-MHz linear array transducer. 2-D guided M-mode images at a 2-mm depth were recorded at the tip of papillary muscles. Posterior and anterior wall thicknesses of the LV chamber and its diameter during systole and diastole were measured in short-axis view using leading edge-to-leading edge convention. All of the parameters were measured over ≥ 3 consecutive cardiac cycles. Ejection fraction was defined as follows: ejection fraction = [(LVEDV - LVESV)/LVESD $\times 100$], where LVEDV is LV end diastolic volume, LVESV is LV end systolic volume, and LVESD is LV end systolic diameter. Fractional shortening was derived as follows: fractional shortening = [(LVEDD - LVESD)/LVEDD $\times 100$], where LVEDD is LV end diastolic diameter. Cardiac output was derived as follows: cardiac output = [(ESV - EDV) \times HR], where ESV is end systolic volume, EDV is end diastolic volume, and HR is heart rate.

Histological Analysis Postmortem

Formalin-fixed, paraffin-embedded tissue sections (6 μ m) were deparaffinized and rehydrated through alcohol and stained with hematoxylin and eosin. For ACE2, sections were incubated with rabbit anti-ACE2 antibody or matched rabbit IgG nonimmune control (Dako) then detected with biotinylated universal secondary

antibodies (1:200), ABC kit, and standard diaminobenzidine staining. For immunofluorescence, heart sections were dual stained with ACE2 and α -sarcomeric actin and detected with goat antirabbit FITC (green) and goat antimouse Alexa 633 (red), respectively. For Picrosirius Red, sections were incubated in Sirius Red F3B (0.1% wt/vol saturated picric acid), washed in 0.01 N HCl, and distilled H₂O. Masson's trichrome stain kit (Sigma) was used. For quantification of staining, pixel intensity was measured using Image Pro-Plus software using methods described previously.²⁹

Statistical Analysis

Comparisons were made using 1-way ANOVA. Statistical analysis was performed in Prism version 4.0 (Graph Pad Software). For all of the tests, $P < 0.05$ is statistically significant following Bonferroni or Tukey's posthoc analysis, and results represent mean values and SEM of the data. Cell measurements were analyzed using the Student *t* test.

Results

In Vitro Assessment of Myocyte Structure

We first assessed the effects of ACE2 overexpression on the structure of isolated primary rabbit myocytes. Adenovirus-mediated gene transfer was used in vitro, because rAAV6 does not transduce myocytes in vitro and induce transgene expression in the necessary time frame because of the requirement for second-strand synthesis. ACE2 was efficiently expressed by Ad5 in isolated rabbit myocytes and resulted in a marked increase in cell hypertrophy (Figure S1A through S1C, available in the online data supplement at <http://hyper.ahajournals.org>).

rAAV6 and rAAV9 Vector Biodistribution and Transduction Profiles in SHRSPs After Intravascular Delivery

We determined the capacity of rAAV6 and rAAV9 vectors to transduce the SHRSP heart after a single systemic injection. Both vectors were efficient, and rAAV6-mediated gene transfer was not modified by VEGF coadministration (Figure 1A and 1B). Levels of gene expression mediated by rAAV6 in mice had previously been found to be enhanced by VEGF coadministration.³⁰ Biodistribution studies were carried out (Figure S2), and vector genomes were quantified by TaqMan and revealed marked differences in vector genome accumulation (Figure 1C). Furthermore, biodistribution of rAAV9-packaged genomes to the kidney was far higher than rAAV6. We, therefore, proceeded with rAAV6 for delivery of ACE2 to the myocardium of SHRSPs in vivo.

Effect on BP

To be packaged into rAAV6 vectors, the ACE2 gene was cloned into an AAV shuttle plasmid and tested for functional expression of the ACE2 gene in COS7 cells (Figure S3). Male rats were injected with rAAV6:ACE2, control vectors, or PBS at 8 weeks of age. A previous study indicated a potentially beneficial effect of ACE2 overexpression on BP.¹⁶ We, therefore, analyzed BP after in vivo ACE2 gene transfer. Enalapril treatment was included as a positive control for BP measurements. PBS and rAAV6:hPLAP control animals showed an equivalent increase in BP over time, characteristic of SHRSP (Figure S4). This rise in systolic BP was significantly attenuated by enalapril and by ACE2 overexpression

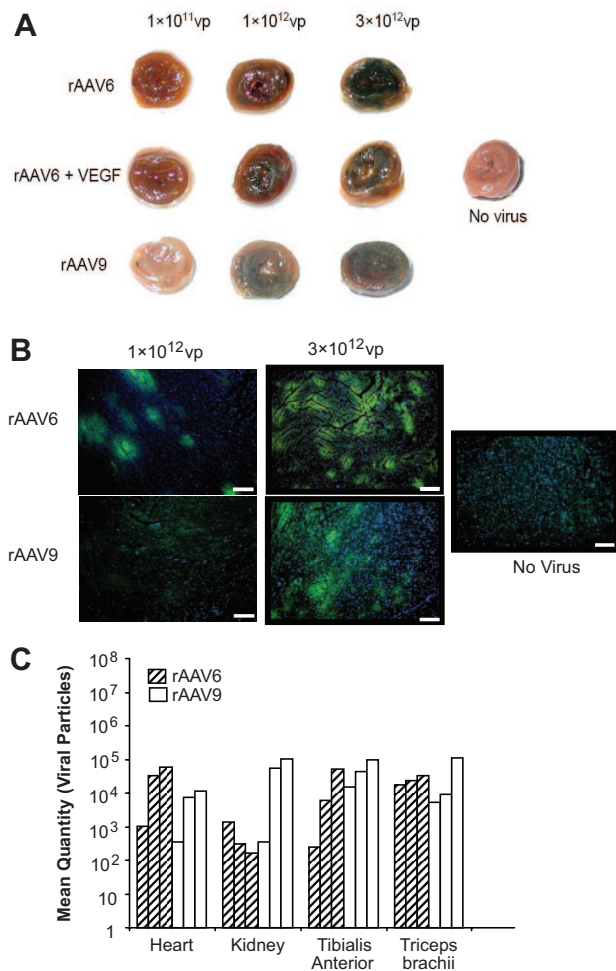


Figure 1. Transduction of cardiac tissue by rAAV6 and rAAV9 vectors. SHRSPs were infused with 3 different doses of rAAV6:CMVlacZ or rAAV9:CMVlacZ (1×10^{11} vp, 1×10^{12} vp, or 3×10^{12} vp). A, Transverse sections of heart tissue fixed and stained for β -galactosidase expression en face were taken 14 days postdelivery of rAAV6, rAAV6+VEGF, or rAAV9 vectors. B, Immunofluorescent detection of β -galactosidase expression with nuclear counterstain DAPI, in heart sections from rAAV6 and rAAV9 vector-transduced animals and PBS-infused control animal. Scale bar=50 μ m. C, Total DNA was extracted from heart, kidney, tibialis anterior, and triceps brachii, and quantitative PCR was performed using lacZ primers. Data are plotted as the mean quantity of viral particles in each tissue analyzed. The 3 bars for each tissue with each virus represent the 3 different doses.

($P < 0.001$). The effects of ACE2 overexpression were especially evident at later time points after injection (Figure S4).

Effect of ACE2 Overexpression on In Vivo Cardiac Function

Our principle aim was to document the effect of long-term ACE2 overexpression on cardiac function during the establishment of hypertension and LV hypertrophy in the SHRSP, which is evident at 12 weeks of age.²⁴ Cardiac function was monitored by echocardiography over the following 11 weeks. LV M-mode echocardiography demonstrated a change in LV diameter and reduction in wall thickness at 4, 8, and 11 weeks postinfusion with reduced systolic function in the rAAV6:ACE2

vector-infused animals compared with PBS, enalapril, and rAAV6:hPLAP vector-infused rats (Figure 2A). M-mode images were used to define wall thicknesses and internal diameters at systole and diastole. Rats treated with rAAV6:ACE2 exhibited a significant (28%) reduction in ejection fraction and also in fractional shortening compared with controls (Table S1 and Figure 2B and 2C). As expected, cardiac output increased with age and body mass in control SHRSPs (Table S1 and Figure 2D). However, no change in cardiac output occurred in rAAV6:ACE2-treated rats (Figure 2D). Furthermore, systolic BP/end systolic volume ratio demonstrated that the rAAV6:ACE2-treated SHRSP showed decreased LV performance (Figure 2E). Interventricular septal wall thickness decreased by 14% in the rAAV6:ACE2 group. There was minimal effect on wall thickness in the rAAV6:hPLAP and PBS groups, and LV mass index did not significantly differ between groups (Figure S5 and Table S1). Echocardiography studies, therefore, revealed that ACE2 overexpression leads to a significant reduction in cardiac function compared with control groups.

Histological Evaluation of Cardiac Structure

Sustained overexpression of ACE2 in rats receiving rAAV6:ACE2 was confirmed at 11 weeks postinjection (Figure 3A). ACE2 overexpression in the heart was colocalized with α -sarcomeric actin expression, confirming that ACE2 overexpression occurred selectively in cardiac myocytes (Figure 3B). ACE2 mRNA was also shown to be upregulated in the hearts of rAAV6:ACE2-treated animals in comparison with rAAV6:hPLAP controls (Figure S6). Clear evidence of cardiac dysregulation in ACE2-expressing hearts was observed with irregular myocyte shape (Figure 3C). The effect of ACE2 on cardiac fibrosis was assessed by Picrosirius Red (Figure 3C) and Masson's trichrome stain (Figure 3C). Myocardial interstitial fibrosis was only observed in the ACE2-expressing SHRSPs (Figure 3C), correlating with the increased expression of collagen I and III in the hearts of rAAV6:ACE2-transduced rats only (Figure S7A and S7B). Expression of gap junction protein connexin 43 was detected between myocytes in all of the groups (Figure 3C). The pattern of connexin 43 staining confirmed the disrupted myocardial organization present in the rAAV6:ACE2-infused animals that was apparent in the hematoxylin and eosin sections (Figure 3C). Endothelial staining with rat endothelial cell marker RECA-1 revealed no obvious evidence of increased angiogenesis in ACE2-treated rats (Figure 3C). Although expression of Ang II was not seen to alter significantly between groups, Ang 1-7 expression was significantly increased in the rAAV6:ACE2-transduced group (Figures 4A, 4B, S7A, and S7B). Collagen I and III expression levels were both significantly increased in the rAAV6:ACE2-transduced group (Figures 4C, 4D, S7C, and S7D). No evidence of increased cardiac apoptosis was found in the hearts of rAAV6:ACE2-transduced animals at the 3-month time point (Figure S8). In assessment of ACE and ACE2 activity in heart lysates from rAAV6:ACE2-transduced animals, ACE2 activity was greater than ACE activity, and both were blocked by incubation with their specific inhibitors (data not shown).

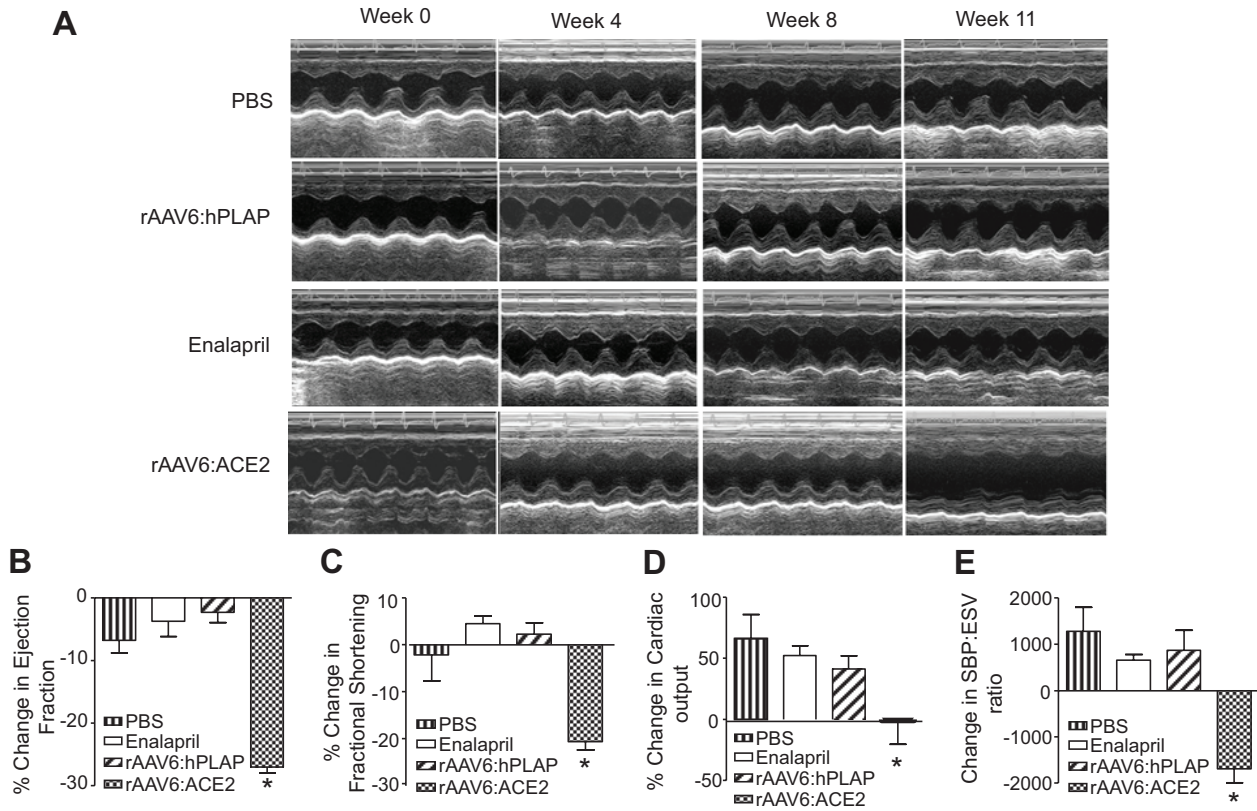


Figure 2. Assessment of cardiac function by echocardiography. Representative traces of M-mode echocardiography at preinfusion and 4, 8, and 11 weeks postinfusion in the 4 experimental groups (A). An ECG trace can be seen along the top of the images. Images from echocardiography carried out at preinfusion and 11-week postinfusion time points were used to calculate (B) percentage change in ejection fraction, (C) change in percentage of fractional shortening, (D) percentage of change in cardiac output, and (E) percentage of change in SB pressure/end systolic volume ratio. * $P < 0.05$ by ANOVA and Tukey's posthoc analysis.

Global Gene Expression Profiling

To assess transcriptional activity in the hearts of animals overexpressing ACE2, we performed gene expression profiling using Illumina expression arrays on animals terminated at 4 weeks postgene transfer. Microarray analysis revealed activation of a profibrotic phenotype at the transcriptional level in ACE2 animals. Fibrosis-associated genes, including collagen type III α 1, fibronectin 1, and lysyl oxidase, were upregulated (Table S2 and Figure S9). Furthermore, genes implicated in the maintenance of cardiac function, including apelin, myosin heavy chain 11, and GATA binding protein 6, were found to be downregulated (Table S2 and Figure S9). The regulation of integrin β 2, fibronectin 1, and myosin heavy chain 11 was assessed in the hearts of rAAV6:ACE2-transduced SHRSPs in comparison with rAAV6:hPLAP-transduced SHRSPs (Figure S10A through S10C). Gene expression data correlated with the pathway shown in Figure S9. These data confirm the activation of transcriptional pathways defining profibrotic effects mediated by myocardial ACE2 delivery in vivo.

Discussion

In the present study, we demonstrate that efficient and sustained (11-week) rAAV6-mediated ACE2 overexpression in myocardium of SHRSPs exerts detrimental effects on cardiac structure and function while lowering BP. Myocardial

changes were characterized by morphological adaptations including severe myocardial interstitial and perivascular fibrosis, an increase in collagen content, and abnormal myocardial organization. The effects of ACE2 overexpression were presumed to be a direct effect on cardiomyocytes as rAAV6 mediates selective gene delivery to cardiomyocytes, confirmed by biodistribution studies and ACE2 expression colocalization studies. However, a disruption in the communication between myocytes and cardiac fibroblasts cannot be ruled out as a potential interaction pertinent to the development of the observed phenotype.

Cardiomyocytes could not be isolated from the hearts of rAAV6:ACE2-transduced SHRSPs to assess hypertrophy at the single-cell level, because the degree of fibrosis made the process of isolation too severe for myocyte survival. However, in vitro studies confirmed that ACE2 overexpression leads to cardiomyocyte hypertrophy. The pivotal role of Ang II in hypertension and LV hypertrophy is well documented. Studies in ACE2-deficient mice¹⁵ showed an increase in systolic BP and elevated plasma levels of Ang II, indicating that ACE2 is key in the metabolism of Ang II. At present, however, the role of ACE2 in the renin-Ang system remains ambiguous. Previous ACE2 intervention studies in mice or rats¹⁶ have shown conflicting results. Crackower et al¹⁴ proposed ACE2 as an essential regulator of heart function. The loss of ACE2 in mice resulted in severe cardiac contrac-

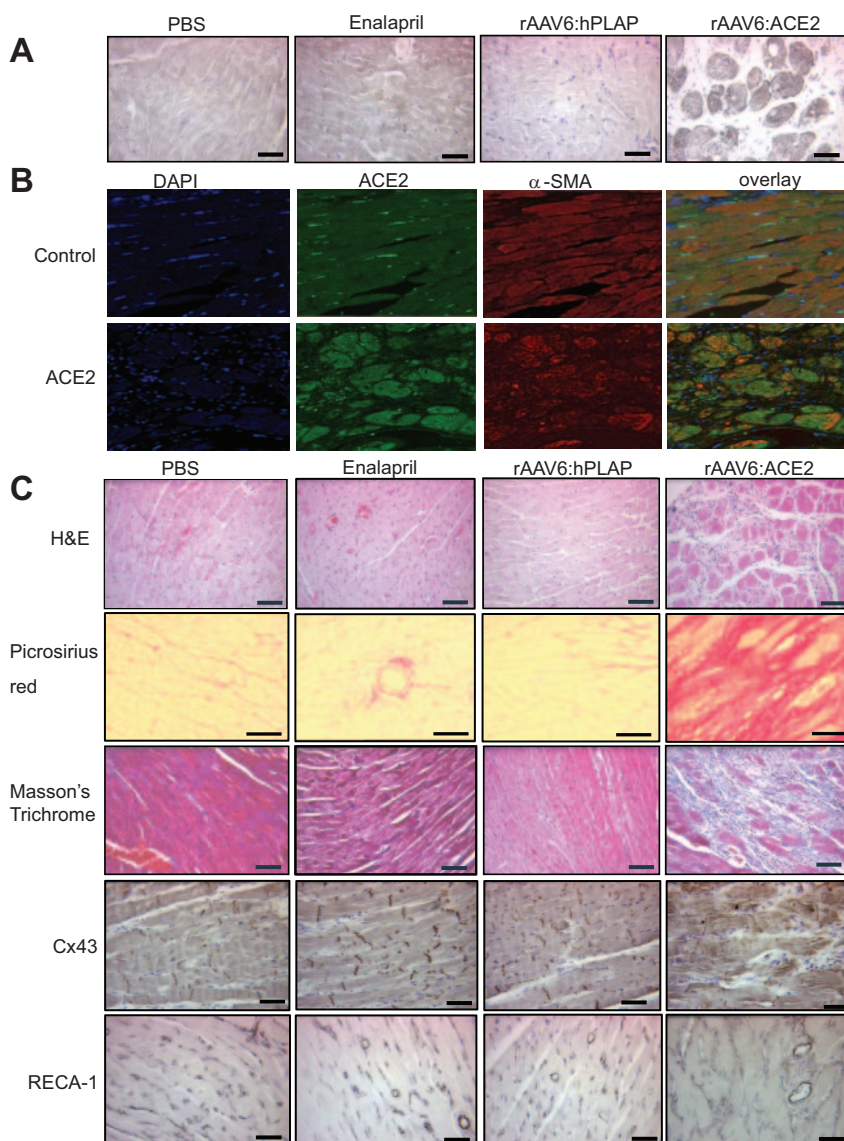


Figure 3. Cardiac histological analysis. Histological analysis was carried out on heart sections at termination at 11-weeks postinfusion ($n=4$). A, Immunohistochemistry with an anti-ACE2 antibody. Scale bar= $100\ \mu\text{m}$; magnification, $\times 40$. B, Dual staining of heart sections with ACE2 and α -smooth muscle actin. (C) Hematoxylin and eosin staining in all groups. Scale bar= $100\ \mu\text{m}$; magnification, $\times 40$. Heart sections were analyzed for fibrosis and collagen content by Picrosirius Red staining. Scale bar= $100\ \mu\text{m}$; magnification, $\times 25$. Masson's trichrome staining. Scale bar= $30\ \mu\text{m}$; magnification, $\times 20$. Connexin 43 staining and RECA-1 staining. Scale bar= $100\ \mu\text{m}$; magnification, $\times 40$.

tility defects and an increase in Ang II levels, indicating that ACE2 controls levels of Ang II *in vivo*.¹⁴ In a separate study, ACE2 gene transfer resulted in significant attenuation of high BP and cardiac fibrosis in the spontaneously hypertensive rat.¹⁶ However, Donoghue et al¹⁷ showed that transgenic mice with increased cardiac ACE2 expression displayed a high incidence of sudden death. In the present study, transduction of cardiomyocytes with both low and high doses of Ad5:ACE2 led to an increase in cell volume. Recently, it has been shown that ACE2 overexpression, followed by permanent coronary artery ligation in rats, resulted in cardiac function preservation.³¹ The BP data in this present study correlate with that of studies in which ACE2 was overexpressed via lentiviral vector delivery.¹⁶ However, it is unlikely to have occurred via the same mechanism. Using lentiviral vectors,¹⁶ expression of ACE2 after intracardiac injection was shown to occur in the kidney through systemic leakage of the vector, whereas the biodistribution patterns of our vector show no evidence of substantial expression in the kidney. Therefore, attenuation of high BP in the

spontaneously hypertensive rat could be because of beneficial effects of ACE2 acting directly to metabolize Ang II into Ang 1-7 in the kidney. The high BP attenuation in the present study could be explained by a beneficial effect of ACE2 acting on the peripheral circulation, because the expression of ACE2 in our study is not limited to the myocardium. This effect could be mediated either as an effect of activation of the Ang 1-7 Mas receptor, which mediates endothelial NO synthase activation and, thus, NO release,³² or indirectly as a consequence of reduced Ang II levels, because Ang II has been shown to activate NAD(P)H oxidases, resulting in reactive oxygen species production, which inactivates NO.^{33,34} However, severe cardiac dysfunction and fibrosis may have lowered BP as a result of diastolic and systolic abnormalities generating cardiac decompensation. Cardiac dysfunction is present from 4 weeks postinfusion, whereas significance in BP differences occurs from 7 weeks postinfusion, suggesting that the underlying cardiac dysfunction precedes the lowered BP.

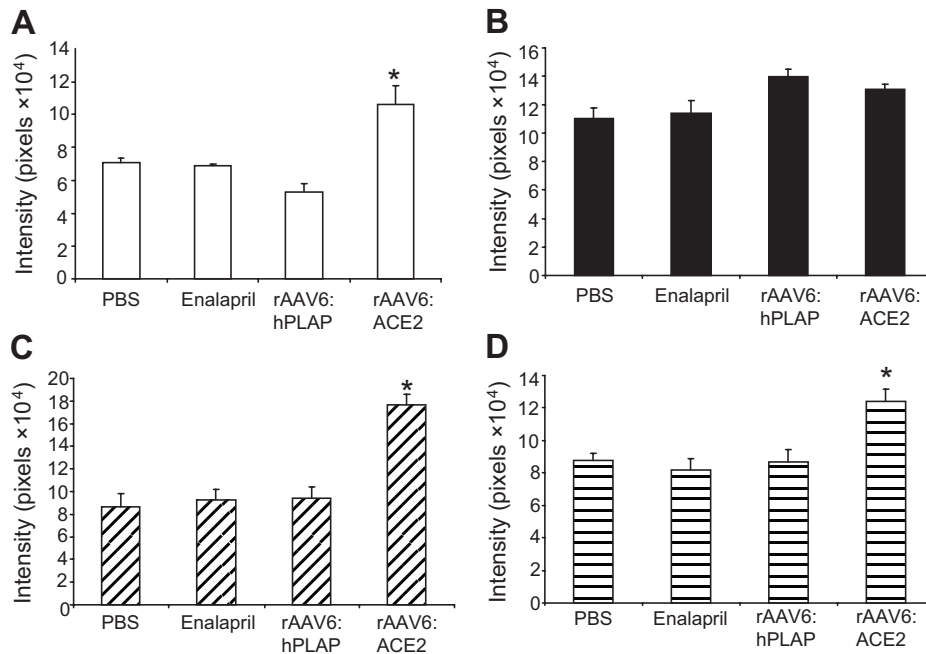


Figure 4. Quantification of histological analysis. Quantification of intensity of staining was carried out for (A) Ang 1-7, (B) Ang II, (C) collagen I, and (D) collagen III. **P*<0.05 vs PBS, enalapril, and rAAV6:hPLAP by ANOVA and Bonferroni's posthoc analysis.

In the study most akin to that described here, local cardiac delivery of a lentiviral vector overexpressing ACE2 resulted in transduction levels of >50% in some areas of the myocardium but to <5% in other areas.¹⁶ Although studies using lentiviral vectors reported reduced BP and beneficial effects on cardiac fibrosis, it is plausible that ACE2 expression levels were not as high as in the present study. Thus, lower ACE2 levels may produce cardioprotective effects while avoiding the induction of detrimental effects on the heart. Transgene dose effects are supported by the occurrence of sudden death earlier in the high ACE2-expressing transgenic mouse line than in the lower-expressing line.¹⁷

Onset of transgene expression from AAV6 in rat has been reported to be evident from 1 week postgene delivery, significantly increasing by 4 weeks and maximal by 12 weeks postgene delivery.³⁵ The temporal profile of rAAV6:ACE2 expression thus correlates with the echocardiography data in the present study, with deterioration of cardiac function being visible at 4 weeks postinfusion and greatest at the end point of 11 weeks postinfusion.

The hearts of the rAAV6:ACE2-treated animals in the present study showed a reduction in ejection fraction and fractional shortening, a decrease in interventricular wall thickness, a decrease in systolic BP/end systolic volume ratio, and no increase in cardiac output overtime, along with histological evidence of severe fibrosis. All of these phenotypes are consistent with severe cardiac dysfunction progressing toward heart failure. This is in agreement with the transgenic mouse study, which also found that overexpression of ACE2 resulted in profound cardiac dysfunction and mild cardiac fibrosis.¹⁷ Cardiac fibrosis is a marker of cardiac failure and contributes to ventricular wall stiffness, impairing cardiac relaxation resulting in impaired ventricular filling and abnormal diastolic function.³⁶⁻³⁸ The pathogenesis of heart

failure inevitably proceeds to dilated cardiomyopathy, in which heart chambers become markedly enlarged and contractile function deteriorates. In early stages, cardiac enlargement is an adaptive process to maintain cardiac output. However, as the heart overcompensates for declining systolic performance, dilation becomes a pathological process. Dilation in the present study, along with decreased wall thickness, would account for the lack of change in LV mass index in the ACE2-transduced SHRSP.

Perspectives

In conclusion, our data demonstrate the development of severe cardiac abnormalities associated with sustained ACE2 overexpression in vivo. Increased expression may result in loss of function of cardioprotective mechanisms. Additional work should address the extent to which these effects are correlated to the ACE2 expression levels to determine whether beneficial effects can be obtained with reduced expression levels or whether the increased expression of ACE2 at any level is deleterious for cardiac morphology and function.

Acknowledgments

We thank Nicola Britton for invaluable help in BP studies and Elisabeth Beattie for invaluable help in echocardiography studies.

Source of Funding

This work was supported by the British Heart Foundation (PG/07/015/22372).

Disclosures

None.

References

1. Zaman MA, Oparil S, Calhoun DA. Drugs targeting the renin-angiotensin-aldosterone system. *Nat Rev Drug Discov.* 2002;1:621-636.

2. Tipnis SR, Hooper NM, Hyde R, Karran E, Christie G, Turner AJ. A human homolog of angiotensin-converting enzyme. Cloning and functional expression as a captopril-insensitive carboxypeptidase. *J Biol Chem*. 2000;275:33238–33243.
3. Soubrier F, Alhenc-Gelas F, Hubert C, Allegrini J, John M, Tregear G, Corvol P. Two putative active centers in human angiotensin I-converting enzyme revealed by molecular cloning. *Proc Natl Acad Sci U S A*. 1988; 85:9386–9390.
4. Ehlers MR, Riordan JF. Angiotensin-converting enzyme: zinc- and inhibitor-binding stoichiometries of the somatic and testis isozymes. *Biochemistry*. 1991; 30:7118–7126.
5. Donoghue M, Hsieh F, Baronas E, Godbout K, Gosselin M, Stagliano N, Donovan M, Woolf B, Robison K, Jeyaseelan R, Breitbart RE, Acton S. A novel angiotensin-converting enzyme-related carboxypeptidase (ACE2) converts angiotensin I to angiotensin 1-9. *Circ Res*. 2000;87: E1–E9.
6. Burrell LM, Risvanis J, Kubota E, Dean RG, MacDonald PS, Lu S, Tikellis C, Grant SL, Lew RA, Smith AI, Cooper ME, Johnston CI. Myocardial infarction increases ACE2 expression in rat and humans. *Eur Heart J*. 2005;26:369–375, discussion 322–364.
7. Vickers C, Hales P, Kaushik V, Dick L, Gavin J, Tang J, Godbout K, Parsons T, Baronas E, Hsieh F, Acton S, Patane M, Nichols A, Tummino P. Hydrolysis of biological peptides by human angiotensin-converting enzyme-related carboxypeptidase. *J Biol Chem*. 2002;277:14838–14843.
8. Levy S. Drug insight: angiotensin-converting-enzyme inhibitors and atrial fibrillation—indications and contraindications. *Nat Clin Pract Cardiovasc Med*. 2006;3:220–225.
9. Kober L, Torp-Pedersen C. Do ACE inhibitors improve outcome in patients with stable vascular disease? *Nat Clin Pract Cardiovasc Med*. 2007;4:124–125.
10. McMurray JJ. Val-HeFT: do angiotensin-receptor blockers benefit heart failure patients already receiving ACE inhibitor therapy? *Nat Clin Pract Cardiovasc Med*. 2005;2:128–129.
11. Gupta M, Lonn EM, Verma S. Should patients with stable coronary artery disease be treated with ACE inhibitor therapy? *Nat Clin Pract Cardiovasc Med*. 2005;2:124–125.
12. Ferrario CM, Chappell MC, Tallant EA, Brosnihan KB, Diz DI. Counter-regulatory actions of angiotensin-(1-7). *Hypertension*. 1997;30: 535–541.
13. Ferrario CM. Angiotensin-(1-7) and antihypertensive mechanisms. *J Nephrol*. 1998;11:278–283.
14. Crackower MA, Sarao R, Oudit GY, Yagil C, Kozieradzki I, Scanga SE, Oliveira-dos-Santos AJ, da Costa J, Zhang L, Pei Y, Scholey J, Ferrario CM, Manoukian AS, Chappell MC, Backx PH, Yagil Y, Penninger JM. Angiotensin-converting enzyme 2 is an essential regulator of heart function. *Nature*. 2002;417:822–828.
15. Gurley SB, Allred A, Le TH, Griffiths R, Mao L, Philip N, Haystead TA, Donoghue M, Breitbart RE, Acton SL, Rockman HA, Coffman TM. Altered blood pressure responses and normal cardiac phenotype in ACE2-null mice. *J Clin Invest*. 2006;116:2218–2225.
16. Diez-Freire C, Vazquez J, Correa de Adjonian MF, Ferrari MF, Yuan L, Silver X, Torres R, Raizada MK. ACE2 gene transfer attenuates hypertension-linked pathophysiological changes in the SHR. *Physiol Genomics*. 2006;27:12–19.
17. Donoghue M, Wakimoto H, Maguire CT, Acton S, Hales P, Stagliano N, Fairchild-Huntress V, Xu J, Lorenz JN, Kadambi V, Berul CI, Breitbart RE. Heart block, ventricular tachycardia, and sudden death in ACE2 transgenic mice with downregulated connexins. *J Mol Cell Cardiol*. 2003;35:1043–1053.
18. Baker AH, Sica V, Work LM, Williams-Ignarro S, de Nigris F, Lerman LO, Casamassimi A, Lanza A, Schiano C, Rienzo M, Ignarro LJ, Napoli C. Brain protection using autologous bone marrow cell, metalloproteinase inhibitors, and metabolic treatment in cerebral ischemia. *Proc Natl Acad Sci U S A*. 2007;104:3597–3602.
19. Inagaki K, Fuess S, Storm TA, Gibson GA, McTiernan CF, Kay MA, Nakai H. Robust systemic transduction with AAV9 vectors in mice: efficient global cardiac gene transfer superior to that of AAV8. *Mol Ther*. 2006;14:45–53.
20. Wang Z, Zhu T, Qiao C, Zhou L, Wang B, Zhang J, Chen C, Li J, Xiao X. Adeno-associated virus serotype 8 efficiently delivers genes to muscle and heart. *Nat Biotechnol*. 2005;23:321–328.
21. Pacak CA, Mah CS, Thattaliyath BD, Conlon TJ, Lewis MA, Cloutier DE, Zolotukhin I, Tarantal AF, Byrne BJ. Recombinant adeno-associated virus serotype 9 leads to preferential cardiac transduction in vivo. *Circ Res*. 2006;99:e3–e9.
22. Gratton JA, Sauter A, Rudin M, Lees KR, McColl J, Reid JL, Dominiczak AF, Macrae IM. Susceptibility to cerebral infarction in the stroke-prone spontaneously hypertensive rat is inherited as a dominant trait. *Stroke*. 1998;29:690–694.
23. Ohtaka M. Stroke-prone SHR (SHRSP) as models for clinical and epidemiological studies on hypertension-related cardiac diseases in humans. *Jpn Circ J*. 1980;44:347–360.
24. Davidson AO, Schork N, Jaques BC, Kelman AW, Sutcliffe RG, Reid JL, Dominiczak AF. Blood pressure in genetically hypertensive rats. Influence of the Y chromosome. *Hypertension*. 1995;26:452–459.
25. McIntyre M, Hamilton CA, Rees DD, Reid JL, Dominiczak AF. Sex differences in the abundance of endothelial nitric oxide in a model of genetic hypertension. *Hypertension*. 1997;30:1517–1524.
26. Kerr S, Brosnan MJ, McIntyre M, Reid JL, Dominiczak AF, Hamilton CA. Superoxide anion production is increased in a model of genetic hypertension: role of the endothelium. *Hypertension*. 1999;33:1353–1358.
27. Yamori Y, Horie R, Handa H, Sato M, Fukase M. Pathogenetic similarity of strokes in stroke-prone spontaneously hypertensive rats and humans. *Stroke*. 1976;7:46–53.
28. Odom GL, Gregorevic P, Chamberlain JS. Viral-mediated gene therapy for the muscular dystrophies: successes, limitations and recent advances. *Biochim Biophys Acta*. 2007;1772:243–262.
29. Hoffman RM, Yang M. Whole-body imaging with fluorescent proteins. *Nat Protoc*. 2006;1:1429–1438.
30. Gregorevic P, Blankinship MJ, Allen JM, Crawford RW, Meuse L, Miller DG, Russell DW, Chamberlain JS. Systemic delivery of genes to striated muscles using adeno-associated viral vectors. *Nat Med*. 2004;10:828–834.
31. Der Sarkissian S, Grobe JL, Yuan L, Narielwala DR, Walter GA, Katovich MJ, Raizada MK. Cardiac overexpression of angiotensin converting enzyme 2 protects the heart from ischemia-induced pathophysiology. *Hypertension*. 2008;51:712–718.
32. Sampaio WO, Souza dos Santos RA, Faria-Silva R, da Mata Machado LT, Schiffrin EL, Touyz RM. Angiotensin-(1-7) through receptor Mas mediates endothelial nitric oxide synthase activation via Akt-dependent pathways. *Hypertension*. 2007;49:185–192.
33. Griendling KK, Minieri CA, Ollerenshaw JD, Alexander RW. Angiotensin II stimulates NADH and NADPH oxidase activity in cultured vascular smooth muscle cells. *Circ Res*. 1994;74:1141–1148.
34. Zhang H, Schmeisser A, Garlich CD, Plotze K, Damme U, Mugge A, Daniel WG. Angiotensin II-induced superoxide anion generation in human vascular endothelial cells: role of membrane-bound NADH-/NADPH-oxidases. *Cardiovasc Res*. 1999;44:215–222.
35. Palomeque J, Chemaly ER, Colosi P, Wellman JA, Zhou S, Del Monte F, Hajjar RJ. Efficiency of eight different AAV serotypes in transducing rat myocardium in vivo. *Gene Ther*. 2007;14:989–997.
36. Brilla CG, Janicki JS, Weber KT. Impaired diastolic function and coronary reserve in genetic hypertension. Role of interstitial fibrosis and medial thickening of intramyocardial coronary arteries. *Circ Res*. 1991; 69:107–115.
37. Doering CW, Jalil JE, Janicki JS, Pick R, Aghili S, Abrahams C, Weber KT. Collagen network remodelling and diastolic stiffness of the rat left ventricle with pressure overload hypertrophy. *Cardiovasc Res*. 1988;22: 686–695.
38. Jalil JE, Doering CW, Janicki JS, Pick R, Shroff SG, Weber KT. Fibrillar collagen and myocardial stiffness in the intact hypertrophied rat left ventricle. *Circ Res*. 1989;64:1041–1050.

ONLINE SUPPLEMENT

Title: ONSET OF EXPERIMENTAL SEVERE CARDIAC FIBROSIS IS MEDIATED BY OVEREXPRESSION OF ACE2

Short Title: Cardiac overexpression of ACE2 leads to fibrosis

Authors: Rachel Masson¹, Stuart A. Nicklin¹, Margaret Anne Craig¹, Martin McBride¹, Kirsten Gilday¹, Paul Gregorevic², James M. Allen², Jeffrey S. Chamberlain², Godfrey Smith³, Delyth Graham¹, Anna F. Dominiczak¹, Claudio Napoli^{4,5} and Andrew H. Baker¹

¹BHF Glasgow Cardiovascular Research Centre, University of Glasgow, 126 University Place, Glasgow, G12 8TA, UK.

²Senator Paul D. Wellstone Muscular Dystrophy Cooperative Research Centre, University of Washington, Seattle, Washington 98195, USA.

³FBLS, West Medical Building, University of Glasgow, G12 8QQ, UK.

⁴Sbarro Institute for Cancer Research and Molecular Medicine, College of Science and Technology, Temple University, Philadelphia, PA 19122, USA.

⁵Department of General Pathology, 1st School of Medicine, II University of Naples, 80138 Naples, Italy.

Corresponding Author: Andrew H Baker, PhD, BHF Glasgow Cardiovascular Research Centre, University of Glasgow, 126 University Place, Glasgow G12 8TA

Fax: +44 (0)1413306997, Tel: +44(0)1413301977, email: ab11f@clinmed.gla.ac.uk

Supplementary Methods

***In Vitro* assessment of myocyte structure**

Adenoviral infection of H9c2 cells, grown in supplemented EMEM, was performed with either Ad5:ACE2 or Ad5:*LacZ* at various multiplicity of infection (MOI). For primary myocytes, New Zealand White rabbits (2-2.5kg) were euthanized and hearts removed and perfused retrogradely (25mlmin^{-1} , 37°C) with a nominally Ca^{2+} free Krebs-Henseleit solution supplemented with 0.6mgml^{-1} collagenase and 0.1mgml^{-1} protease for 6 minutes. Myocytes were counted and adenoviral infection performed during seeding at 3×10^4 cells/dish with either Ad5:ACE2 or Ad5:*LacZ*. Myocytes were cultured in supplemented M199 medium (Sigma) for 48 hours. Cell volume was calculated using a graticule (n=50).

ACE and ACE2 Activity Assay

ACE and ACE2 activity were determined using an assay based on the use of Fluorogenic Peptide Substrate VI (FPS VI) (R&D Systems, Minneapolis, USA). ACE and ACE2 cleave an amide bond between the fluorescent group and the quencher group (Pro and Lys), resulting in an increase in fluorescence in the presence of ACE and ACE2 activity at excitation and emission spectra of 320 and 405 nm, respectively. Briefly, heart were lysed using lysis buffer (75 mM Tris pH 7.5, 1 M NaCl, and $0.5\ \mu\text{M}$ ZnCl_2) and the protein content determined by BCA. Samples were normalised to an arbitrary quantity and made up to $50\ \mu\text{l}$. To the samples the following was added; $100\ \mu\text{M}$ FPS VI, $10\ \mu\text{M}$

ACE inhibitor captopril and reaction buffer (1 M NaCl, 75 mM Tris and 0.5 mM ZnCl₂, pH 7.5) in a final volume of 100 µl.

To determine specific ACE2 activity, the experiment was also carried out in the presence of 100 µM ACE2 inhibitor DX600 (Phoenix Pharmaceuticals, Inc, California, USA).

Fluorescence was monitored every 50 seconds for 2500 seconds using a spectrophotometer (Spectramax, Molecular Devices).

Histological Analysis

Formalin-fixed paraffin-embedded tissue sections (6µm) were sequentially deparaffinised and rehydrated through an alcohol gradient. For collagen 1, collagen III, Ang II and Ang 1-7 expression analysis, sections were incubated with relevant antibody or matched rabbit IgG nonimmune control (Dako, Denmark) followed by detection with biotinylated universal secondary antibody (1/200), ABC Kit and standard diaminobenzidine staining. Sections were counterstained with haematoxylin.

Taqman gene expression analysis

Total RNA was isolated from heart tissue at termination (4 weeks post-infusion) following treatment with rAAV6:hPLAP or rAAV6:ACE2. cDNA was synthesised using a QPCR cDNA synthesis kit (Stratagene, CA, USA) as per manufacturer's instructions. Expression of ACE2 was confirmed by Taqman™ Q-RT-PCR using an ACE2 taqman gene expression assay (Applied Biosystems). Probes for integrin beta 2 (ITB2),

fibronectin-1 (FN1) and myosin heavy chain 11 (MYH11) were used to assess regulation of the relevant genes.

Tunel assay

Formalin-fixed paraffin-embedded tissue sections (6 µm) were sequentially deparaffinised and rehydrated through an alcohol gradient. Sections were digested in 5 µg/ml proteinase K at room temperature for 15 minutes then incubated with reaction mixture (0.01mM dATP, 0.01mM biotin-16-dUTP, 50U Tdt) for 1 hour at 37 °C. Endogenous peroxidase was blocked in 3% H₂O₂ before standard diaminobenzidine staining and haematoxylin counterstaining was carried out.

Illumina Gene Expression Profiling

2 groups of animals (n=6) were included in the rAAV6:ACE2 overexpression study. Male 8 week old SHRSP received 3×10^{12} vp of either rAAV6:hPLAP or rAAV6:ACE2 and hearts were excised 4-weeks post-infusion. Total RNA from heart samples was isolated using RNA mini kit from Qiagen according to the manufacturers instructions (Qiagen GmbH, Germany). The quality of total RNA was checked using the total RNA Nano chip assay on an Agilent 2100 Bioanalyzer (Agilent Technologies, Germany). RNA concentrations were determined using the NanoDrop spectrophotometer (Labtech International, U.K.).

Whole-genome-gene expression was assessed using a direct hybridisation approach. Biotin-labeled cRNA samples for hybridization were prepared according to Illumina's recommended sample labelling procedure. Total RNA isolated from tissue underwent a

single round of in vitro (IVT) transcription using the TotalPrep™ RNA Labeling Kit (Ambion, Texas). 500ng of total RNA was used for complementary DNA synthesis, followed by an amplification/labelling step to synthesize biotin-labeled cRNA. Purified cRNA was quality controlled on an Agilent 2100 Bioanalyser and spectrophotometrically quantified.

The labelled sample was then hybridised, washed and stained to each BeadChip. The focused Sentrix Illumina Beadchips, comprising 12 microarrays were scanned on an Illumina BeadArray Reader at a wavelength of 532nm and resolution of less than 1micron. Data was captured using Beadscan vers3.5.3.1 and analysed with Beadstudio 3.1.1.0 software (Illumina Inc, San Diego). The Bead arrays contained a 50mer gene-specific probe to a 29mer address oligo which were in turn randomly assembled on each array containing > 1.6 million pits and generating an average 30 fold redundancy for each sequence represented. The 29-base address was used to map and decode the array, while the probe was used to quantify gene expression levels of transcripts. The RatRef-12 expression BeadChip contained approx. 22,000 probes per array, as selected from the National Centre for Biotechnology Information Reference Sequence database.

In addition to the gene-specific beads, each array also contained control beads (>1000), which allowed all steps in the process to be monitored for sample quality, labelling success rate, hybridisation stringency and signal generation. Illumina Beadstudio software also reported the performance of controls.

Quality controlled Illumina microarrays were normalised using the rank invariant algorithm and the resulting data further analysed using Ingenuity Pathway analysis.

Data was submitted to the ArrayExpress database, accession number E-TABM-613.

Table S1. Echocardiography findings

Group	Week	%EF	%FS	CO (ml/min)	LVMI (mg/g)	RWT	% IVSWT	SBP:ESV	HR (b/min)
PBS	0	88.0 ± 1.5	53.0 ± 2.3	168.6 ± 1.6	2.48 ± 0.1	0.54 ± 0.02	45.0 ± 1.9	2314 ± 433	405.8 ± 1.9
	11	81.3 ± 1.1	50.8 ± 4.1	234.5 ± 18.5	2.96 ± 0.1	0.60 ± 0.01	44.3 ± 3.1	3600 ± 382	375.7 ± 4.0
rAAV6:hPLAP	0	84.5 ± 1.3	49.0 ± 1.7	183.5 ± 7.8	2.51 ± 0.1	0.55 ± 0.02	41.5 ± 3.5	1965 ± 126	428.9 ± 19.9
	11	82.3 ± 1.3	51.3 ± 2.5	233.2 ± 17.8	2.86 ± 0.1	0.60 ± 0.03	43.3 ± 3.5	2842 ± 458	377.2 ± 7.5
rAAV6:ACE2	0	89.0 ± 1.7	55.0 ± 3.2	205.8 ± 2.2	2.84 ± 0.3	0.49 ± 0.01	48.7 ± 1.8	2277 ± 341	393.4 ± 2.6
	11	62.0 ± 2.7*	34.3 ± 4.9*	204.9 ± 17.6*	2.62 ± 0.2	0.49 ± 0.01	33.7 ± 4.4*	582 ± 57*	372.2 ± 9.2
Enalapril	0	84.3 ± 1.3	51.5 ± 0.3	179.1 ± 6.7	2.37 ± 0.1	0.52 ± 0.02	47.5 ± 1.9	2343 ± 159	385 ± 8.7
	11	80.5 ± 2.1	56.0 ± 1.5	231.3 ± 10.1	2.31 ± 0.1	0.57 ± 0.01	42.25 ± 1.3	3003 ± 257	411 ± 4.0

EF, ejection fraction; FS, fractional shortening; CO, cardiac output; LVMI, left ventricular mass index; RWT, relative wall thickness; IVSWT, interventricular septal wall thickness; SBP:ESV, ratio of systolic blood pressure to end systolic volume; HR, heart rate. *p<0.05 rAAV6:ACE2 vs. PBS, Enalapril and rAAV6:hPLAP.

Table S2. Global Gene Expression Profiling – Illumina microarray analysis data revealed altered expression of a range of genes. This table lists fold changes and difference (diff.) scores of 25 of the most up-regulated and down-regulated genes for rAAV6:ACE2 vs rAAV6:hPLAP.

TargetID	Treated Diff.Score	Fold Change	TargetID	Treated Diff.Score	Fold Change
MYH11	-44.402	0.68	MGC105649	81.292	3.03
NGRN	-36.449	0.51	GM2A	83.869	1.93
PENK-RS	-35.57	0.66	LR8	83.903	1.76
RGD1564924	-34.341	0.69	RT1-BA	84.348	2.95
CARD9	-30.291	0.72	CCL2	84.997	1.68
LOC498920	-26.808	0.69	APOBEC1	85.106	2.83
DSCR1L1	-26.339	0.76	MAFB	86.205	1.73
MGC72973	-26.339	0.66	MSR2	89.544	3.07
FGF12	-23.251	0.7	RBP1	94.602	1.88
KCNE1	-23.045	0.42	LOC498279	98.696	1.84
ES2	-22.311	0.58	SPON1	103.278	1.97
HRC	-21.992	0.77	SSG1	104.136	1.69
LOC497785	-21.901	0.75	DCIR3	106.825	2.28
LOC686087	-21.412	0.75	RT1-DB1	110.579	2.45
RGD1304931	-21.377	0.77	FN1	114.972	1.76
NOV	-20.963	0.56	CD68	340.818	2.23
CAT	-20.508	0.75	CTSS	340.818	1.93
SLC9A3R2	-20.508	0.6	CXCL16	340.818	2.05
MYOM2	-19.702	0.78	LCPI	340.818	1.93
DLST	-19.417	0.76	LOC498335	340.818	6.41
LOC498122	-19.138	0.56	LTBP2	340.818	1.99
APLN	-19.134	0.63	POSTN	340.818	2.1
SYPL	-19.134	0.78	SPP1	340.818	2.08
THBD	-18.817	0.75	THBS4	340.818	2.16
RGD1549725	-18.715	0.77	TIMP1	340.818	2.3

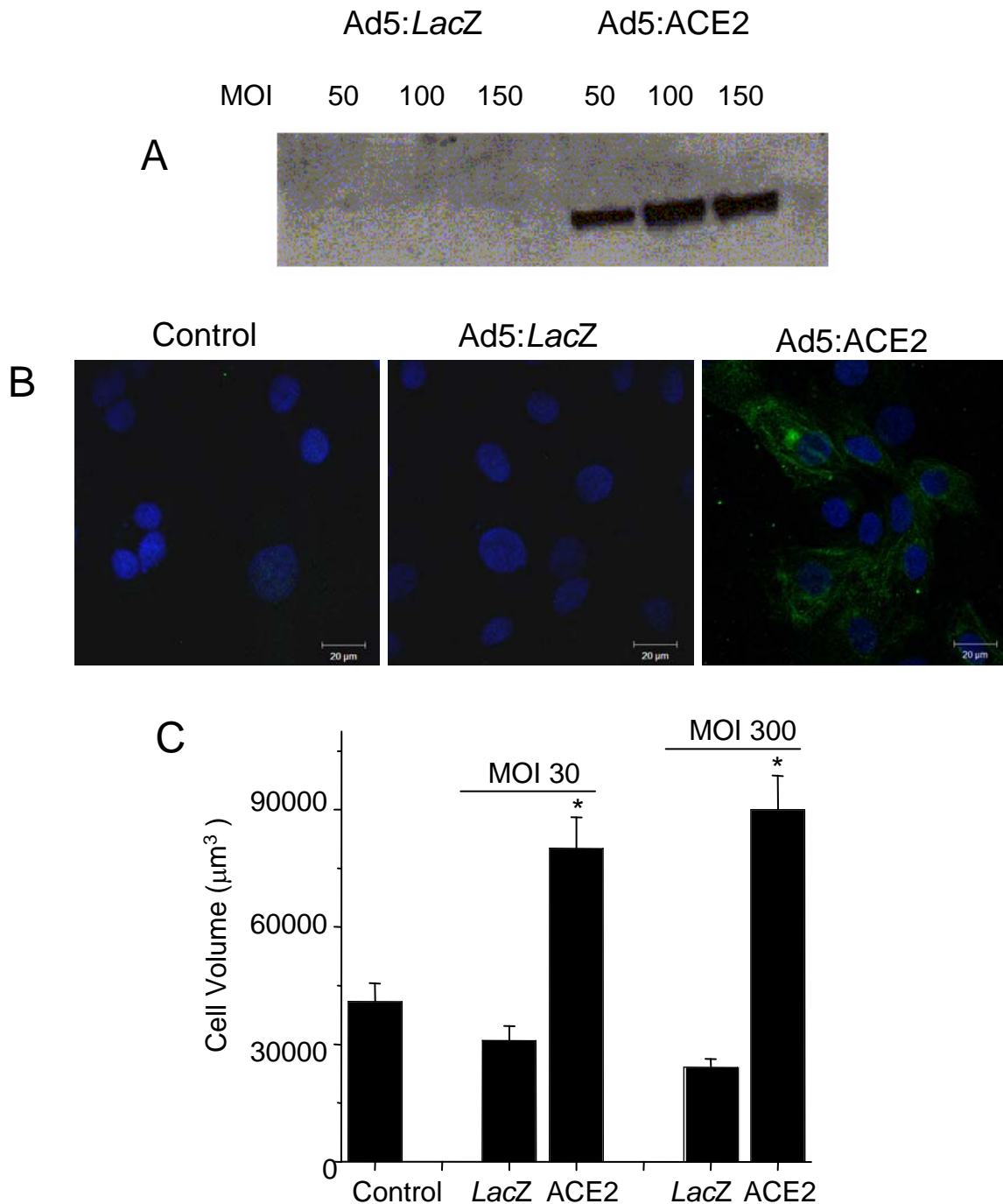


Figure S1 *In vitro* effects of ACE2 overexpression on cell hypertrophy

(A) Western blot analysis of extracts from infected H9c2 cells to show ACE2 overexpression by adenovirus-mediated gene delivery. Cells were infected with a MOI of 50, 100 and 150 pfu/cell. (B) Immunocytochemical localisation of ACE2 to the cell surface in H9c2 cells (C) Isolated single cells were transduced with either Ad5:ACE2 or Ad5:*LacZ* and cell dimensions quantified. Transduction with Ad5:ACE2 resulted in significantly increased cell volume of isolated rabbit myocytes (n=50/group). * p<0.05 vs control and Ad5:*LacZ* infected cells.

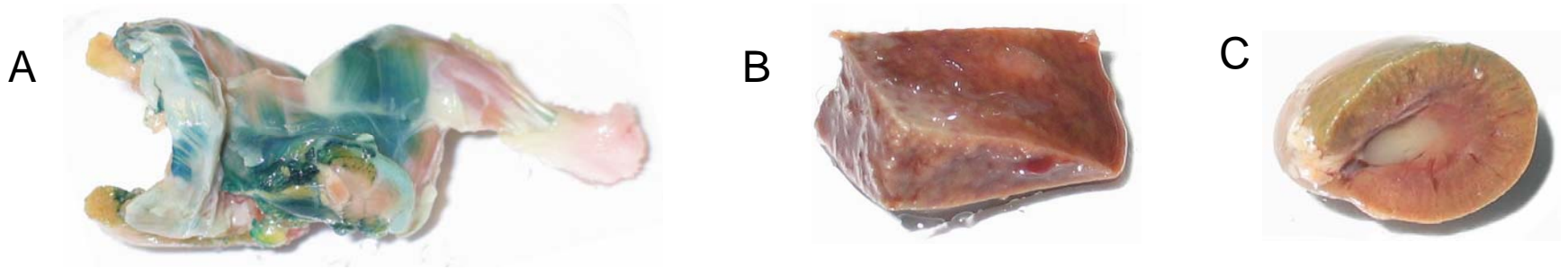


Figure S2 rAAV6:CMVlacZ gene transfer to non-cardiac tissue.

rAAV6:CMVlacZ vectors (3×10^{12} vp/rat) were infused into 6 week old SHRSP rats (n=1). (A) Skeletal muscle, (B) liver and (C) kidney were stained for β -galactosidase after 14 days.

Downloaded from https://academic.oup.com/ascg/advance-article-abstract/doi/10.1093/ascg/19.000/10.000

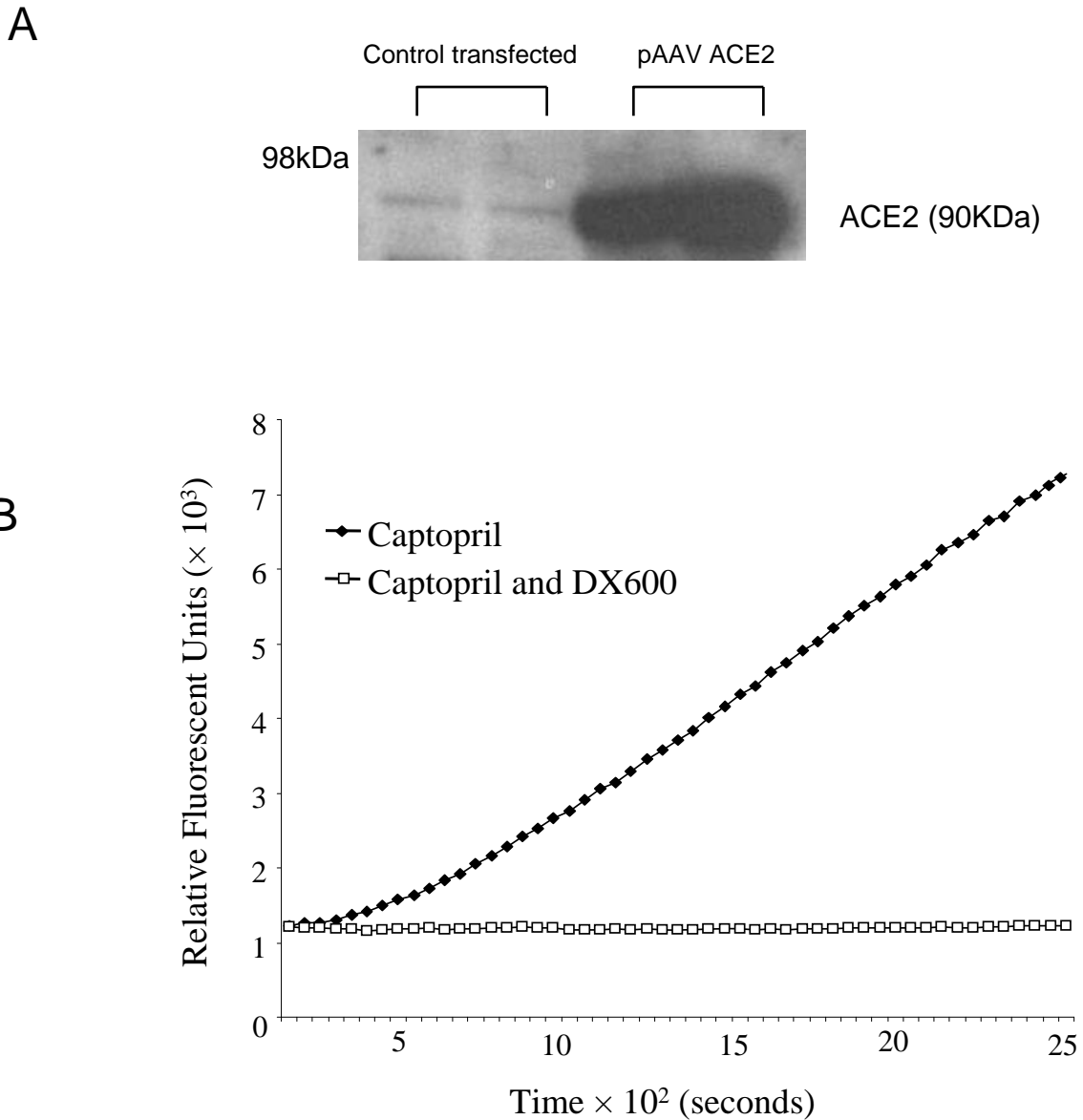


Figure S3 Confirmation of functional ACE2

Cells were transfected with pAAV-ACE2. 48 hours after lipofectamine transfection, cells were harvested and lysed. (A) Cell lysates were subjected to western immunoblotting and detected with an anti-ACE2 antibody on a 12% gel under reducing conditions. (B) ACE2 activity was measured in the presence of captopril and DX600.

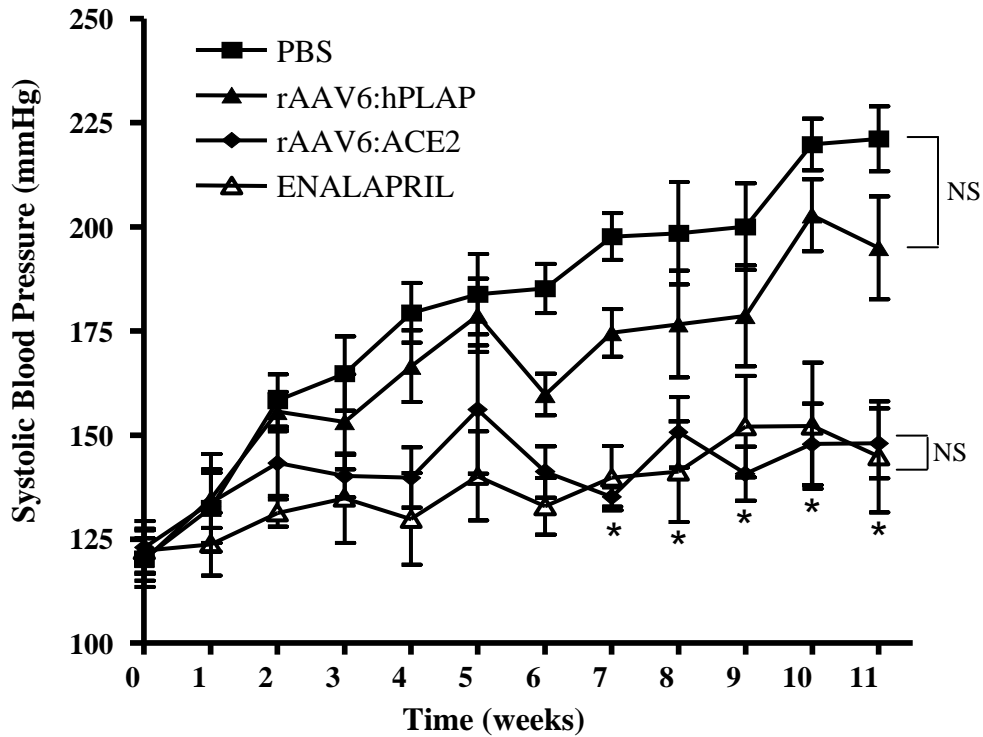


Figure S4 Effect of overexpression of ACE2 on systolic blood pressure

Animals were infused with either rAAV6:hPLAP, rAAV6:ACE2, PBS or treated with Enalapril. Systolic blood pressure was measured weekly by tail cuff. Data are presented as mean \pm SE. * $p < 0.001$ rAAV6:ACE2 and Enalapril vs. PBS and rAAV6:hPLAP, as determined by ANOVA analysis and Bonferroni test.

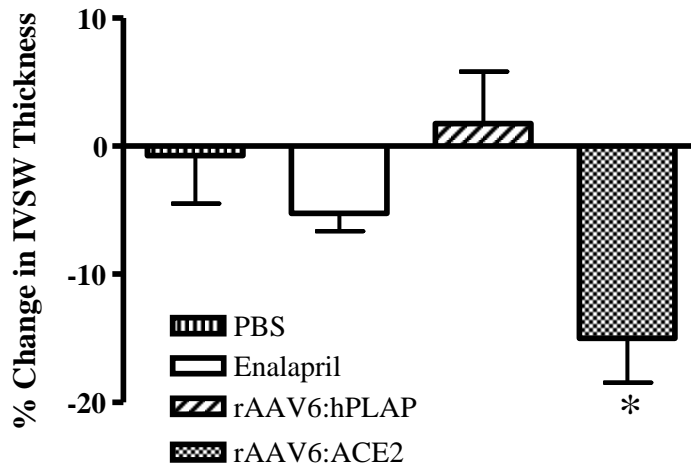


Figure S5 Interventricular septal wall thickness

Echocardiography was carried out pre-infusion and at 11 weeks post-infusion on rAAV6:hPLAP, PBS, Enalapril and rAAV6:ACE2 treated animals. Images were used to calculate % change in interventricular septal wall thickness. * $p < 0.05$ by ANOVA and Tukey's post hoc analysis.

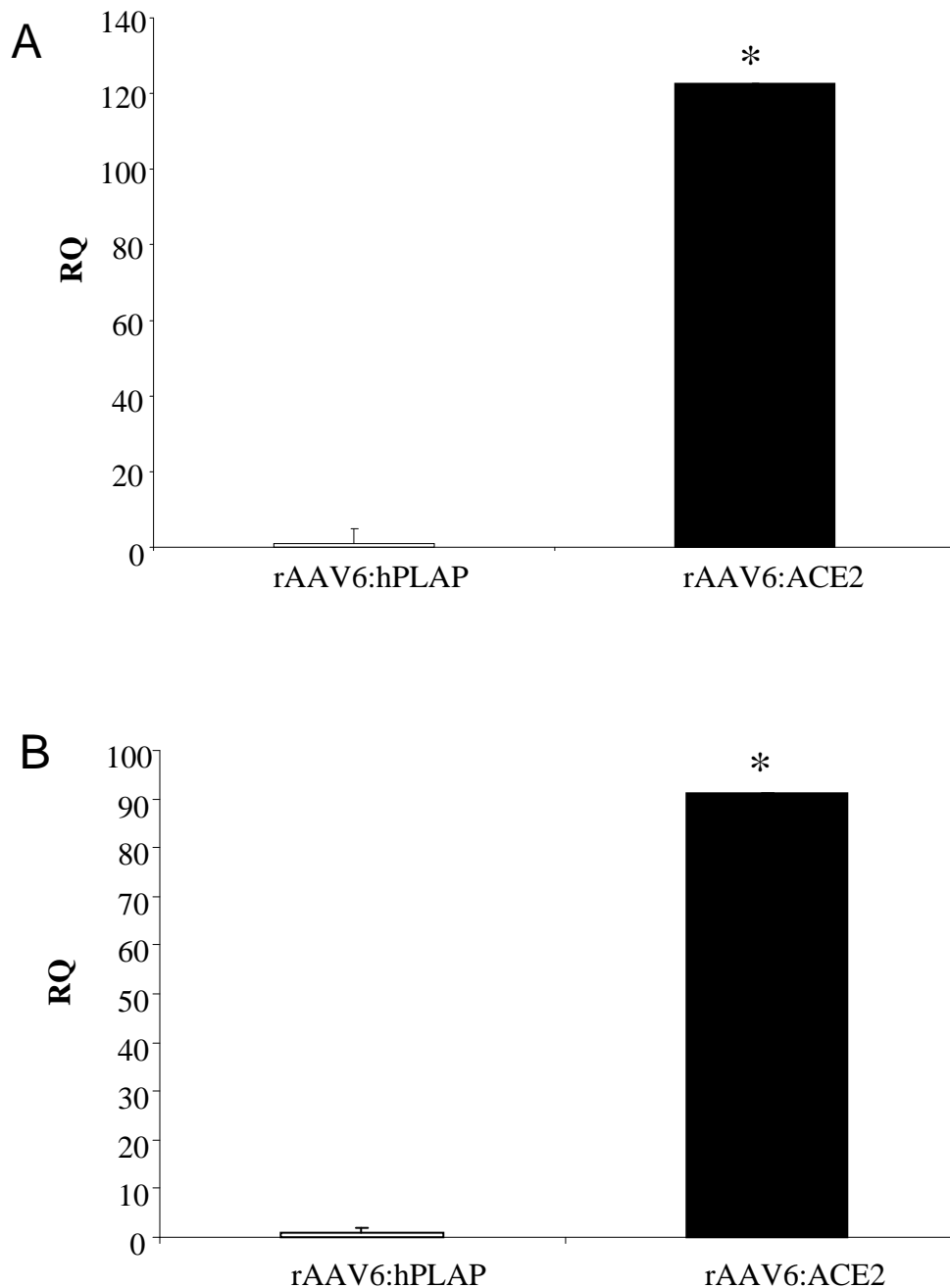


Figure S6 Quantification of ACE2

Total RNA was isolated from heart tissue at termination at (A) 4 weeks post-infusion and (B) 11 weeks post-infusion following treatment with rAAV6:hPLAP or rAAV6:ACE2 and taqman gene expression analysis performed to quantify ACE2 mRNA. Data are presented as fold change (RQ). * $p < 0.05$ vs rAAV6:hPLAP by students t-test.

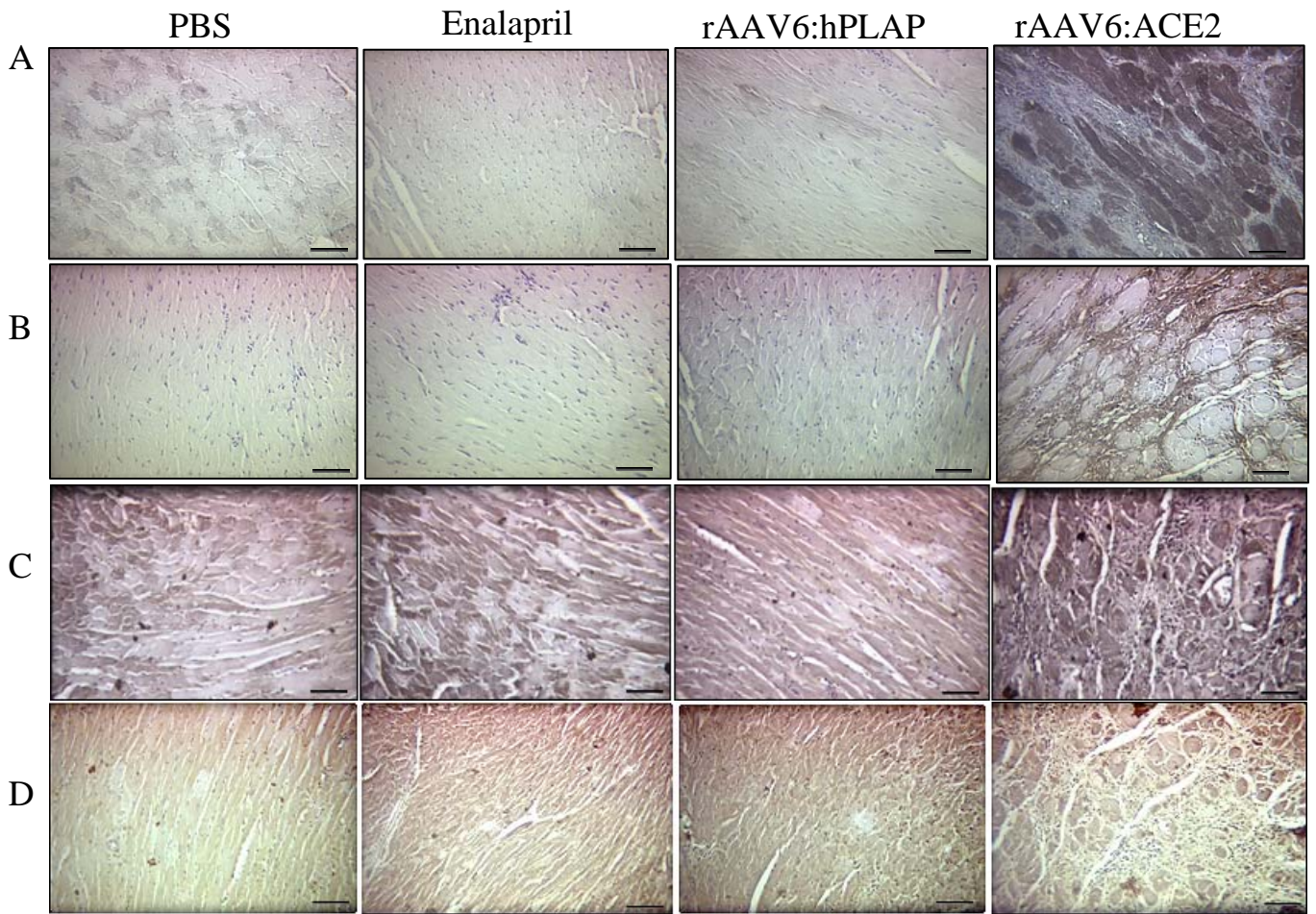


Figure S7 Histological Analysis

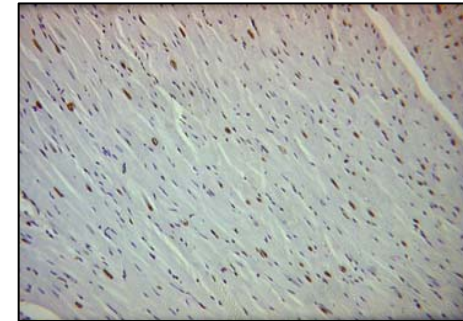
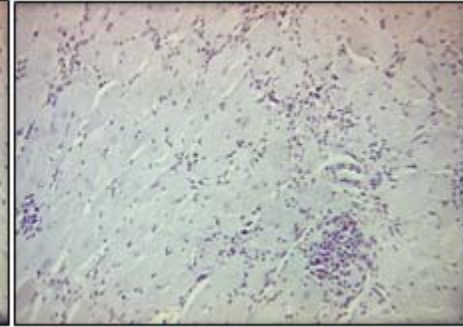
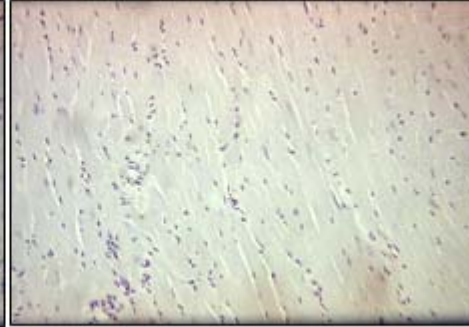
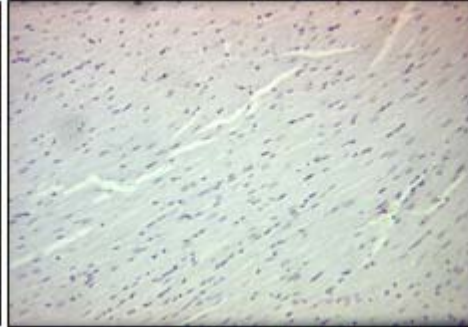
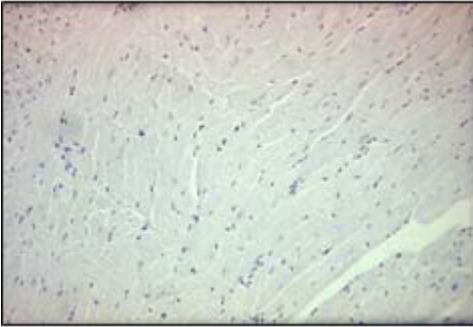
Histological analysis was carried out on heart sections at termination (n=4). (A) Immunohistochemistry with (A) an anti-Collagen I antibody, (B) anti-collagen III antibody, (C) anti-Ang 1-7 antibody and (D) anti-Ang II antibody. Scale bar = 30µm, magnification × 20.

PBS

Enalapril

rAAV6:hPLAP

rAAV6:ACE2



Positive
control

Figure S8 Assessment of cardiac apoptosis

Terminal deoxynucleotidyl transferase dUTP nick end labeling (Tunel) was carried out on heart sections taken at termination from PBS, Enalapril, rAAV6:hPLAP and rAAV6:ACE2 transduced animals.

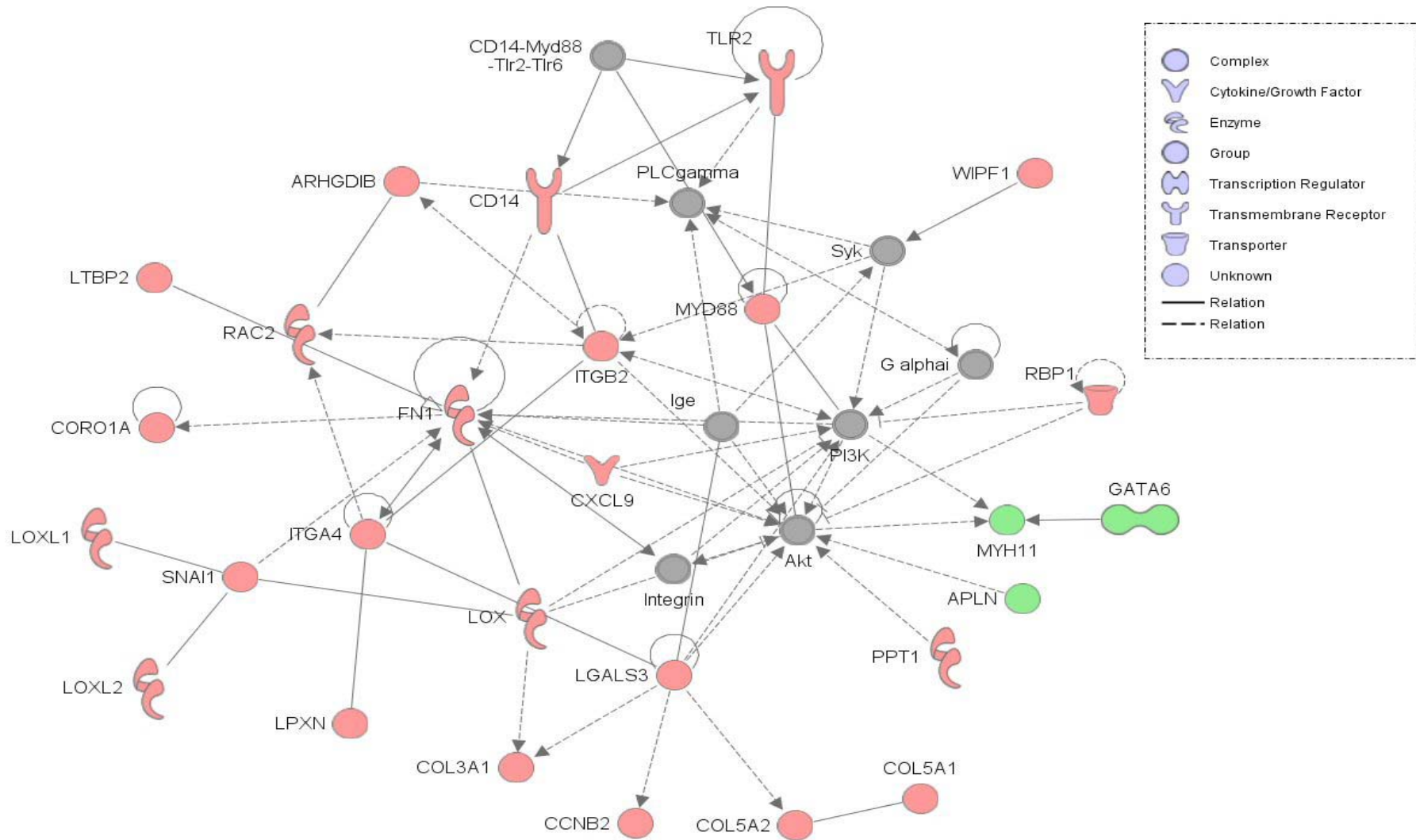


Figure S9 Gene expression profiling

Total RNA was isolated from heart tissue at termination (4 weeks post-infusion) following treatment with rAAV6:hPLAP or rAAV6:ACE2 and Illumina microarray analysis performed. Ingenuity pathway analysis revealed the dysregulation of a number of genes and pathways. The most altered pathway is shown. Red indicates gene up-regulation for rAAV6:ACE2 vs rAAV6:hPLAP, whilst green represents gene down-regulation for rAAV6:ACE2 vs rAAV6:hPLAP. Grey represents unchanged genes.

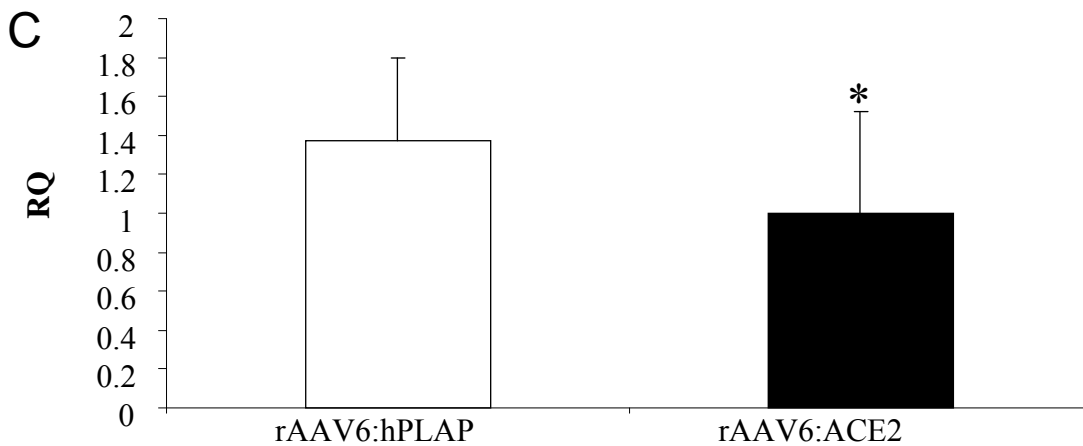
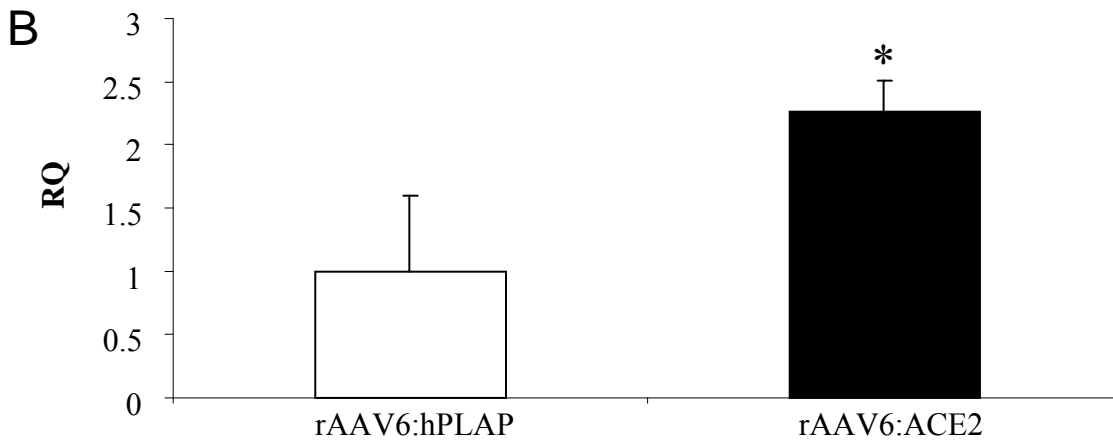
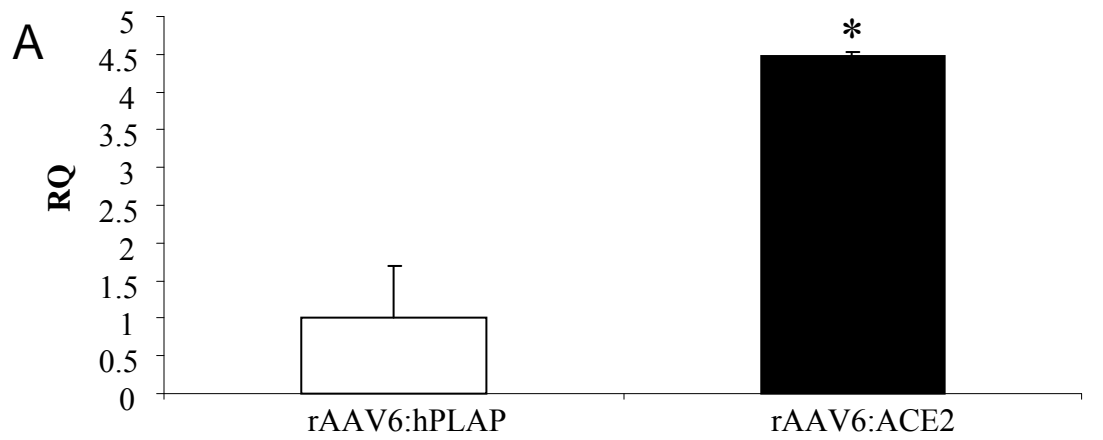


Figure S10 Taqman gene expression analysis

Total RNA was isolated from heart tissue at termination (4 weeks post-infusion) following treatment with rAAV6:hPLAP or rAAV6:ACE2 and taqman gene analysis performed with probes for (A) Integrin β 2 (ITB2), (B) Fibronectin 1 (FN1) and (C) Myosin heavy chain 11 (MYH11). * $p < 0.05$ vs rAAV6:hPLAP by students t-test.